ADVANCED MATERIALS INTERFACES
www.advmatinterfaces.de

Sphere-on-Tube Biomimetic Hierarchical Nanostructures Coupled with Engineered Surfaces for Enhanced Photoelectrochemical Biosensing of Cancer Cells Expressing Folate Receptors

Ning Gao, Xueying Wang, Jinhui Feng, Xiaojian Li, Huan Wang, Dawei Fan, Yong Zhang, Hongmin Ma, Qin Wei,* and Huangxian Ju*

The quantitative detection of cancer cells and the evaluation of folate receptor (FR) expression on cell membranes are of great significance for tumor-related research. In this work, a photoelectrochemical (PEC) biosensing interface is proposed for detection of cancer cells based on the construction of nanostructured platforms coupled with surface engineering. A "sphere-on-tube" hierarchical nanostructure is fabricated by depositing biomimetic polydopamine nanospheres on TiO_2 nanotube arrays. Enhanced PEC responses are achieved with the formation of polyethylene glycol antifouling layers and the immobilization of folic acid as a recognition ligand. Based on the ligand–receptor interaction, the antifouling PEC biosensor exhibits a wide linear range for the detection of the breast cancer cell line MDA-MB-231 from 20 to 2.0×10^6 cells mL^{-1} with a low detection limit of 15 cells mL^{-1} (S/N = 3). The expressing differentiation of FR on several cancer cells is well discriminated. The proposed PEC cytosensing method shows great potential in detection of cancer cells expressing folate receptors.

1. Introduction

The overexpressed protein receptors on tumor cell surfaces play important roles in tumorigenesis and metastasis of cancers.[1–3] It is critical to understand the roles of membrane receptors in disease development and it is appealing to develop methods for evaluation of their expressing levels on cancer cells.[4] Cytosensors are attractive methods for cancer cells sensing due to the high sensitivity and the label-free sensing mode.[5,6] A variety of cytosensing strategies, including electrochemical,[7–10] electrochemiluminescence,[11–13] photoelectrochemical (PEC),[14–16] quartz crystal microbalance,[17] and surface plasmon resonance,[18] have been proposed for the detection and evaluation of cell membrane receptors. Among these label-free sensing technologies, PEC cytosensors possess the advantages of low background signal and thus high sensitivity due to the unique photo-to-current transforming process. For the binding of membrane receptors, biorecognition elements such as antibodies and aptamers should be incorporated into the sensing platform.[19] Based on the high binding affinity between ligands and protein receptors, the ligands have been used as recognition probes for the construction of cytosensing interfaces.[20]

Folate receptor (FR) is one type of membrane proteins overexpressed on tumor cells of several malignant cancers and has been well used as a target for imaging and treatment of cancers.[21] While the most cancers are heterogeneous, the expressing levels of folate receptor are closely related to the metastatic phenotypes.[22] Cytosensors for detection of cancer cells expressing folate receptors have been fabricated based on the high affinity between folic acid (FA) and FR.[23,24] Nanomaterials also play important roles in the construction of cytosensing interfaces because they act not only as the transducing elements for signal generation but also as platforms for the immobilization of FA.[25] In consider of the membrane topology of cancer cells,[26] hierarchical nanostructures are promising for capture and sensing of cancer cells.[27] TiO_2 nanotube arrays (TNAs) with highly ordered porous structures are attractive platforms for development of PEC biosensors.[28–32] However, the preparation of hierarchical nanostructures on TNAs for PEC cytosensing has less been reported.

While the evaluation of membrane receptors by cytosensors is based on the capture of cancer cells on sensing interfaces through the recognition effect of immobilized ligands, nonspecific surface interactions should be strictly controlled, especially for the case of cytosensing on porous structures. Cytosensors with antifouling interfaces have been fabricated to

N. Gao, Dr. X. Wang, J. Feng, X. Li, Dr. H. Wang, Dr. D. Fan, Dr. Y. Zhang, Prof. H. Ma, Prof. Q. Wei, Prof. H. Ju
Collaborative Innovation Center for Green Chemical Manufacturing and Accurate Detection
Key Laboratory of Interfacial Reaction and Sensing Analysis in Universities of Shandong
School of Chemistry and Chemical Engineering
University of Jinan
Jinan 250022, P. R. China
E-mail: chm_mahm@ujn.edu.cn; chm_weiq@ujn.edu.cn

The ORCID identification number(s) for the author(s) of this article can be found under https://doi.org/10.1002/admi.202100421.

DOI: 10.1002/admi.202100421

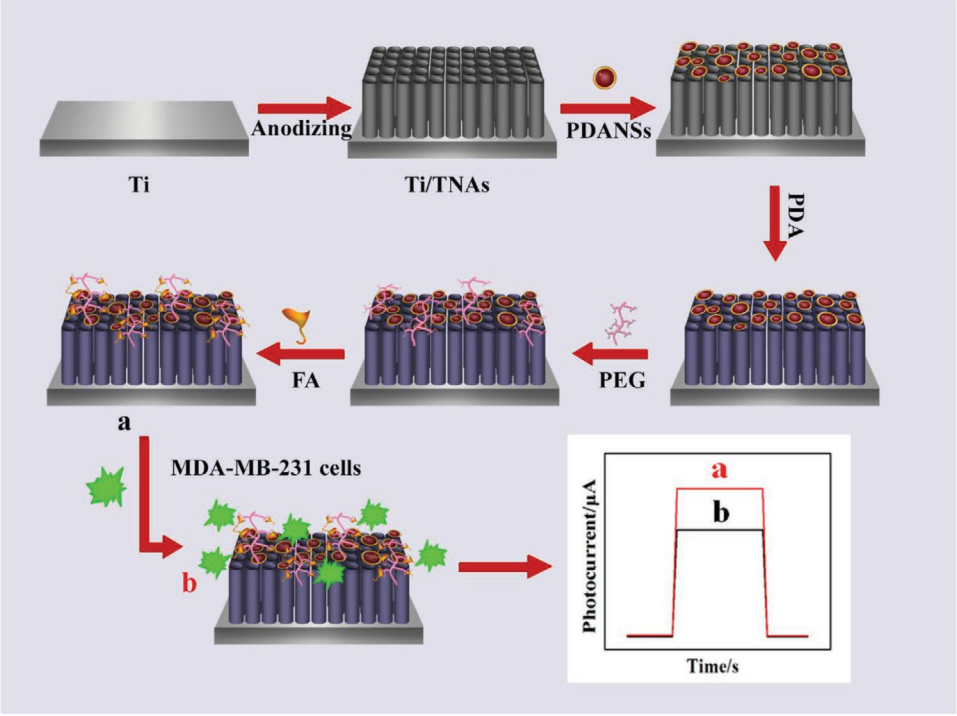

Scheme 1. Schematic illustration of preparation of PEC biosensor.

reduce the nonspecific cell adsorption.[33,34] In this work, hierarchical nanostructures were combined with antifouling interfaces for the development of a PEC cytosensor (**Scheme 1**). A "sphere-on-tube" hierarchical nanostructure was fabricated by depositing biomimetic polydopamine nanospheres (PDANSs) on TNAs. Further polydopamine (PDA) coating was performed to enhance the visible light response and the photo-to-current converting efficiency.[35,36] The sensing interface was finally achieved by the construction of antifouling layers and the conjugation of FA.[37] The fabricated hierarchical nanostructures show enhanced cytosensing performances and the expression of FR on several cancer cells was discriminated.

2. Results and Discussion

2.1. Formation of "Sphere-on-Tube" Hierarchical Nanostructures

TNAs prepared by anodic oxidation can be easily transformed to the anatase form (Figure S3A, Supporting Information) through calcination and show good PEC performances. Furthermore, the unique porous structures with adjustable pore diameters (**Figure 1**A) are excellent platforms for the fabrication of hierarchical nanostructures. A "sphere-on-tube" hierarchical structure (Figure 1C) was created by decoration of polydisperse melanin-like PDANSs (Figure 1B) on TNAs. The abundant catechol groups on PDANSs enable the facile attachment on the surface of TNAs based on the coordination interaction with the titanium atoms.[38,39] In our previous work, we have reported the functionalization of TNAs with mussel-inspired PDA surface coating.[37] The PEC responses under visible light was greatly enhanced due to the formation of complex of electron transfer. In spite of the homology with PDA films, PDANSs decorated on TNAs show little enhancement effect on PEC responses due to the low coverage and contact area, which will be discussed below. For the subsequent surface engineering, PDA coatings were further deposited on prepared hierarchical nanostructures to form a consistent surface functionality and to improve the PEC responses (Figure 1D). Moreover, the surface composition change of composite coating can be further determined by Fourier transform infrared spectra (Figure S3B, Supporting Information). It can be noticed that the sharp peaks at 1591 and 3435 cm^{-1} were assigned to the aromatic rings and catechol −OH of polydopamine.[40] The peaks at 1693 and 1632 cm^{-1} can be attributed to the stretching vibrations of the C=O group of −COOH and amide group of folic acid.[41,42] Respectively, the peak at 1604 cm^{-1} belonged to the bending vibrations of the N−H group. Therefore, the characteristic absorption peak further confirmed the incorporation of PEG and FA.

2.2. Surface Engineering for Construction of PEC Sensing Interfaces

The grafting of antifouling layers on nanostructured platforms was combined with the immobilization of recognition ligands to construct a sensing interface. The quinone structures in PDA coatings show high reactivity toward amino groups by Michael addition or Schiffbase reaction.[33,43] Furthermore, PDA enhances the photoelectric response of TiO_2 by improving the separation of photoinduced electron hole pairs and two OH groups of the catechol moiety can form a strong bidentate complex with coordinatively unsaturated Ti atoms.[44] An antifouling layer was constructed by grafting amino-terminated eight-arm

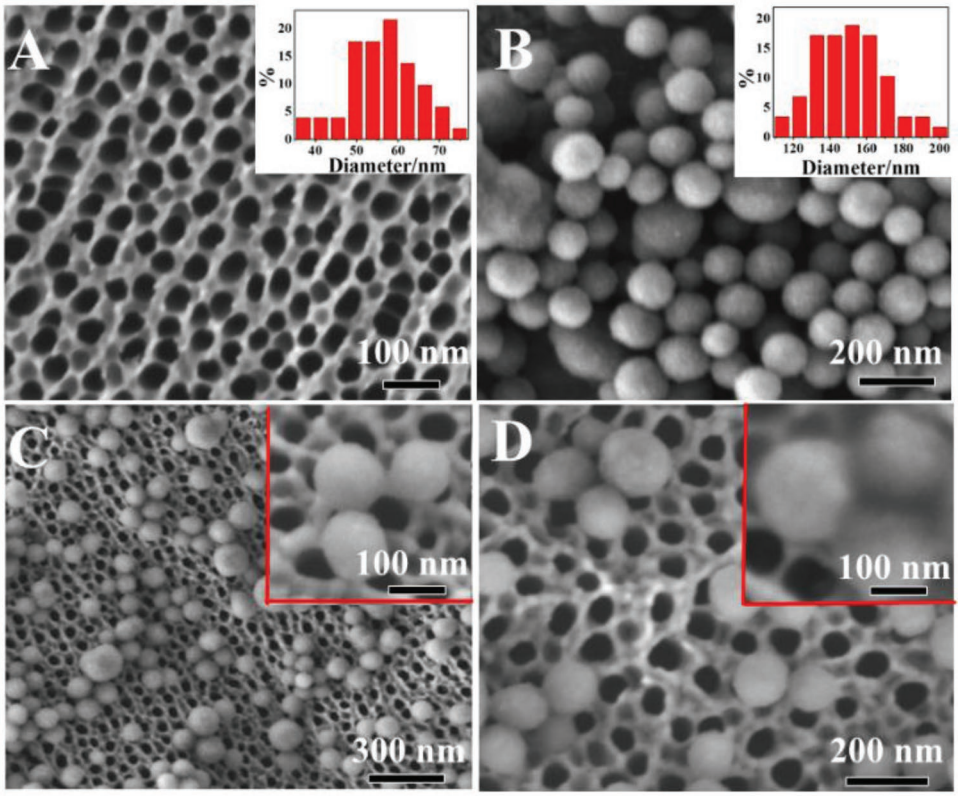

Figure 1. SEM images of A) TNAs, B) PDANSs, C) TNAs/PDANSs, and D) TNAs/PDANSs/PDA.

PEG onto PDA coating. Meanwhile, the remaining amino groups on branched PEG was further immobilized FA as a recognition element. The change of surface functionality during the engineering process was accompanied by the change of wetting properties, which was easily evaluated by measuring the contact angle (CA). The static water CA of titanium pieces was 38.6 (±1.3)° (**Figure 2**A). Moreover, the static water CA of TNAs was become 19.4 (±1.6)° (Figure 2B).[45] The static water CA of TNAs/PDANSs electrode was 16.3 (±1.5)° (Figure 2C). The static water CA of TNAs/PDANSs/PDA electrode was 30.4 (±1.1)° (Figure 2D). Notably, the static water CA of TNAs/PDANSs/PDA/PEG electrode reduced to 8.7 (±1.2)° (Figure 2E). After modifying the FA on the TNAs/PDANSs/PDA/PEG electrode, the static water CA of the PEC biosensor interface was 15.2 (±1.7)° (Figure 2F).

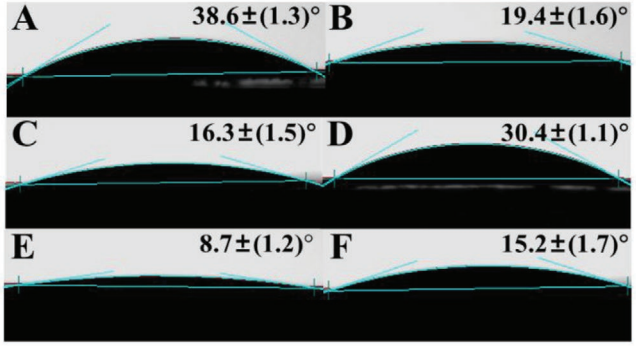

Figure 2. Hydrostatic contact angle of the electrodes: A) Ti, B) TNAs, C) TNAs/PDANSs, D) TNAs/PDANSs/PDA, E) TNAs/PDANSs/PDA/PEG, and F) TNAs/PDANSs/PDA/PEG-FA.

2.3. Characterization of PEC Platform

The modification process of PEC platform and the successful surface engineering can be further confirmed by electrochemical impedance spectrum (EIS).[46] **Figure 3**A shows the impedance spectra of different modified electrodes related to each construction step of the biosensor and the inset is the corresponding equivalent circuit. The R_{et} value of TNAs electrode was large (curve a), which was related to the characteristics of semiconductor materials. However, the R_{et} value of the TNAs/PDANSs electrode (curve b) was decreased. Moreover, the R_{et} value of TNAs/PDANSs/PDA was very small (curve c), owing to the charge transfer characteristics of PDA. With the modification of PEG (curve d) and FA (curve e), the R_{et} values of the electrodes gradually increase due to the hinder effect of electron transfer.[47,48] Figure 3B manifested the photocurrent at different modification stages. It can be found that the TNAs in anatase form have good photoelectric properties (curve a). After modifying PDANSs (curve b), the photocurrent was increased. The further PDA coating induces a significant increase of photocurrent owing to enhanced PEC response (curve c).[49,50] The grafting of PEG (curve d) and conjugation of FA (curve e) induce the decreases of photocurrent. In addition, the introduction of PEG layers and FA molecules hinders the electron transfer of the AA donor in the solution.

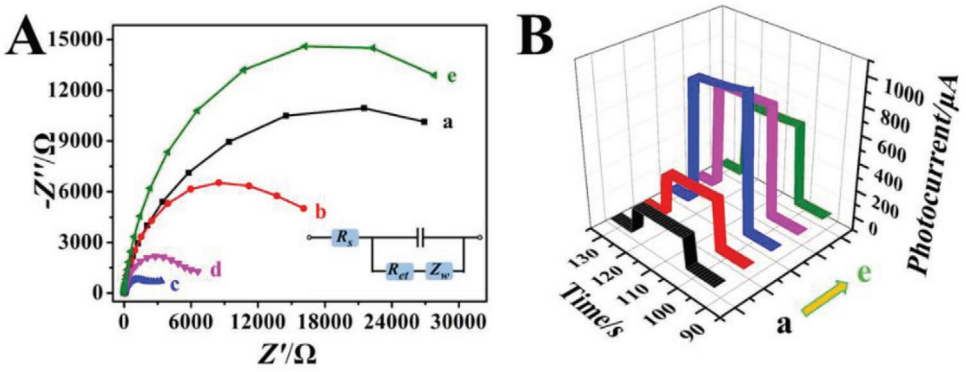

Figure 3. A) EIS and B) photocurrent responses of the different modified electrodes: a) TNAs, b) TNAs/PDANSs, c) TNAs/PDANSs/PDA, d) TNAs/PDANSs/PDA/PEG, and e) TNAs/PDANSs/PDA/PEG-FA. Inset of part (A): the electrical equivalent circuit applied to fit the impedance spectra.

This hindering effect mediated photocurrent change is also mode of the signal response for the sensing of cancer cells.

2.4. Antifouling Performance of PEC Biosensing Interfaces

The fouling effect of bovine serum albumin (BSA) was used to study the antifouling performance of the fabricated biosorption interfaces. The adhesive properties of PDA result in the adsorption of BSA and significant fouling effect (**Figure 4**A). As is expected, due to the antifouling performance of the PEG layers, the R_{et} value had barely change (Figure 4B). The antifouling performance was well retained after the conjugation of FA (Figure 4C), which forms the bases for the specific recognition of FA receptors and reduces the nonspecific adsorption of cancer cells. In consistent with EIS tests, when the TNAs/PDANSs/PDA electrode was soaked in the BSA solution the photocurrent was reduced (Figure 4D). Compared with TNAs/PDANSs/PDA electrode in photocurrent, the TNAs/PDANSs/PDA/PEG electrode (Figure 4E) and TNAs/PDANSs/PDA/PEG-FA electrode (Figure 4F) basically unchanged. This demonstrates that PEC biosensing possessed excellent antifouling performance.

2.5. Selectivity, Stability, and Reproducibility of the PEC Biosensor

MDA-MB-231 cells are human breast cancer cell lines expressing FR and are selected as targets for the investigation of cytosensing performances. Based on the antifouling ability of the fabricated PEC sensing electrodes toward common proteins, the selectivity investigation was conducted for detection of MDA-MB-231 cells using proteins as interfering substances. The photocurrents of PEC electrodes soaked in the cell single solution or the cell protein mixed solution and protein were almost unchanged (**Figure 5**A), indicating the anti-interference performance of the PEC biosensor was outstanding. The current stability test of the PEC electrodes modified with MDA-MB-231 cell (5.0×10^5 cells mL^{-1}) within 600 s was recorded to detect the output signal stability of the biosensor, and the results were shown in Figure 5B. It can be seen that there was no obvious fluctuation in the light response, the calculated relative standard deviation (RSD) of the photocurrent value was 1.2% (n = 15), indicating the developed PEC biosensor has excellent stability. Repeatability reflects the reliability of the PEC biosensor. Under the same conditions, the photocurrents of five TNAs/PDANSs/PDA/PEG-FA electrodes modified with MDA-MB-231 cells

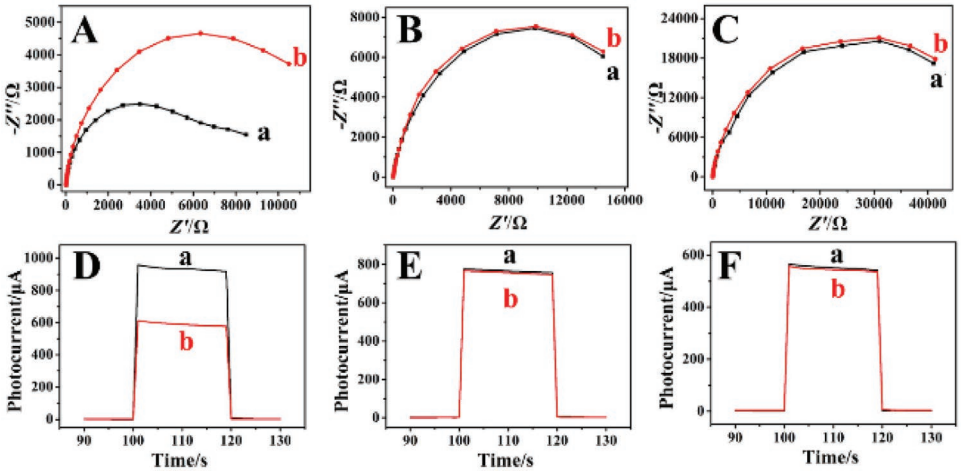

Figure 4. EIS and photocurrent responses of different modified electrodes a) before and b) after immersing in 0.5 mg mL^{-1} BSA solution: A,D) TNAs/PDANSs/PDA, B,E) TNAs/PDANSs/PDA/PEG, and C,F) TNAs/PDANSs/PDA/PEG-FA.

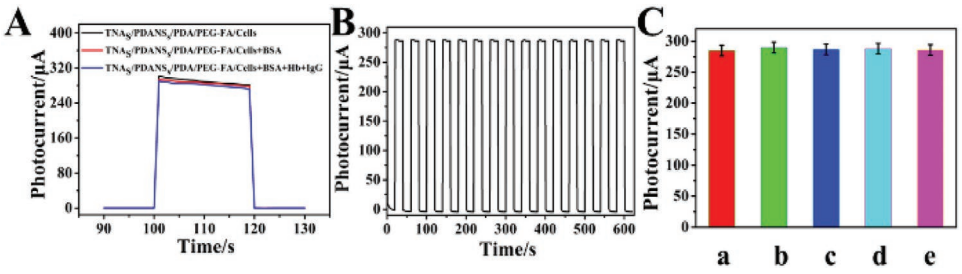

Figure 5. A) The photocurrent test of TNAs/PDANSs/PDA/PEG-FA electrodes soaking in the MDA-MB-231 cell (5.0×10^5 cells mL^{-1}) solution, the mixed solution of MDA-MB-231 cell (5.0×10^5 cells mL^{-1}) and BSA (0.5 mg mL^{-1}), and the mixed solution of MDA-MB-231 cell (5.0×10^5 cells mL^{-1}), BSA (0.5 mg mL^{-1}), Hb (0.5 mg mL^{-1}), and IgG (0.5 mg mL^{-1}). B) The current stability test of 15 on/off lamp cycles of TNAs/PDANSs/PDA/PEG-FA electrode modified with cells (5.0×10^5 cells mL^{-1}). C) The current reproducibility test of five TNAs/PDANSs/PDA/PEG-FA electrodes (a-e) modified with cells (5.0×10^5 cells mL^{-1}).

(5.0×10^5 cells mL^{-1}) were compared to estimate the reproducibility (Figure 5C). The calculated RSD was 2.1%, indicating the PEC biosensor also showed good reproducibility.

2.6. Hierarchical Structure Enhanced PEC Responses of Cancer Cells

While the engineered surfaces show recognition abilities toward MDA-MB-231 cells, the PEC responses to different concentrations of cells were investigated (**Figure 6**A). To demonstrate the advantages of the prepared hierarchical structures for the improving of sensing performances, contrast PEC electrodes without the deposition of PDANSs (TNAs/PDA/PEG-FA) were also prepared and PEC responses were compared with that of TNAs/PDANSs/PDA/PEG-FA (Figure 6B). Based on the hindering effect of the fixed cells on the electron transfer, the photocurrent signals gradually decrease with the increase of the cell concentration of the soaking solution, indicating the direct relationship between the fixed number of cells on electrode and the concentration of the soaking solution. A linear relationship for these PEC responses could be fitted in the range of 20–2.0×10^6 cells mL^{-1}. The linear regression equation obtained with TNAs/PDANSs/PDA/PEG-FA electrode was $\Delta I = 38.99 \lg c + 28.94$ ($R^2 = 0.9934$) and the limit of detection (LOD) was calculated to be 15 cells mL^{-1}. In contrast, the linear regression equation obtained with TNAs/PDA/PEG-FA electrode was $\Delta I = 26.33 \lg c + 14.97$ ($R^2 = 0.9825$), and the LOD was calculated to be 25 cells mL^{-1} (Signal/Noise, S/N = 3).

The obviously enhanced sensing parameters indicate the advantages of the prepared hierarchical nanostructures for the recognition and capturing of cells. The enhanced capturing efficiency could be confirmed by the state of the living cells and the density of the fixed cells on different electrodes. As revealed by fluorescent imaging (**Figure 7**), under the same experimental conditions, the cell density of MDA-MB-231 cells on TNAs/PDANSs/PDA/PEG-FA is larger than that on TNAs/PDA/PEG-FA. Moreover, the cells on TNAs/PDANSs/PDA/PEG-FA can stretch more filopodia (Figure 7D). These filamentous pseudopods exposed more contact areas and adhere to the surface, which can greatly improve the cell capture ability.[47] The cell morphologies on TNAs/PDANSs/PDA/PEG-FA revealed by SEM are also more complete and stretched than that on TNAs/PDA/PEG-FA (**Figure 8**). These results confirm the contributions of the hierarchical structures on the enhanced PEC responses of cancer cells.

2.7. Evaluation of FR Expressing Differentiation on Different Cells

The expressing differentiation of FR mediated the difference between cancer cells and normal tissue cells and also the

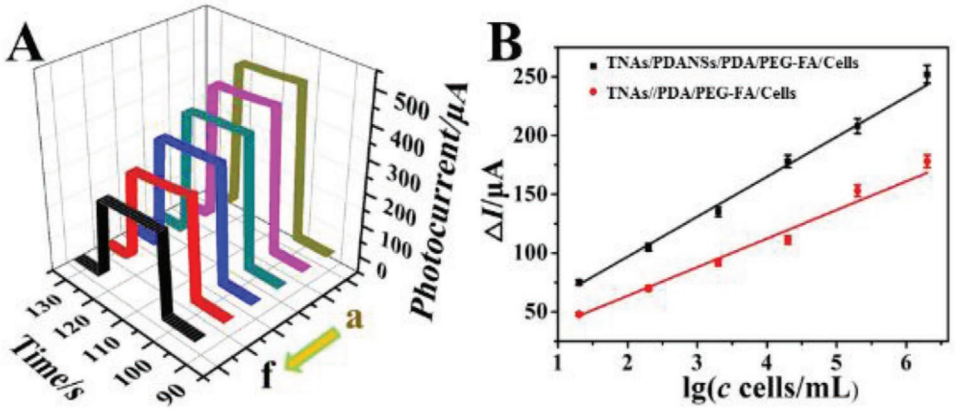

Figure 6. A) The photocurrent response of TNAs/PDANSs/PDA/PEG-FA electrodes at different concentrations: 20, 2.0×10^2, 2.0×10^3, 2.0×10^4, 2.0×10^5, and 2.0×10^6 cells mL^{-1}. B) The linear relationship between photocurrent and logarithm of the cells concentration of the TNAs/PDANSs/PDA/PEG-FA/Cells (black curve) and the TNAs/PDA/PEG-FA/Cells (red curve).

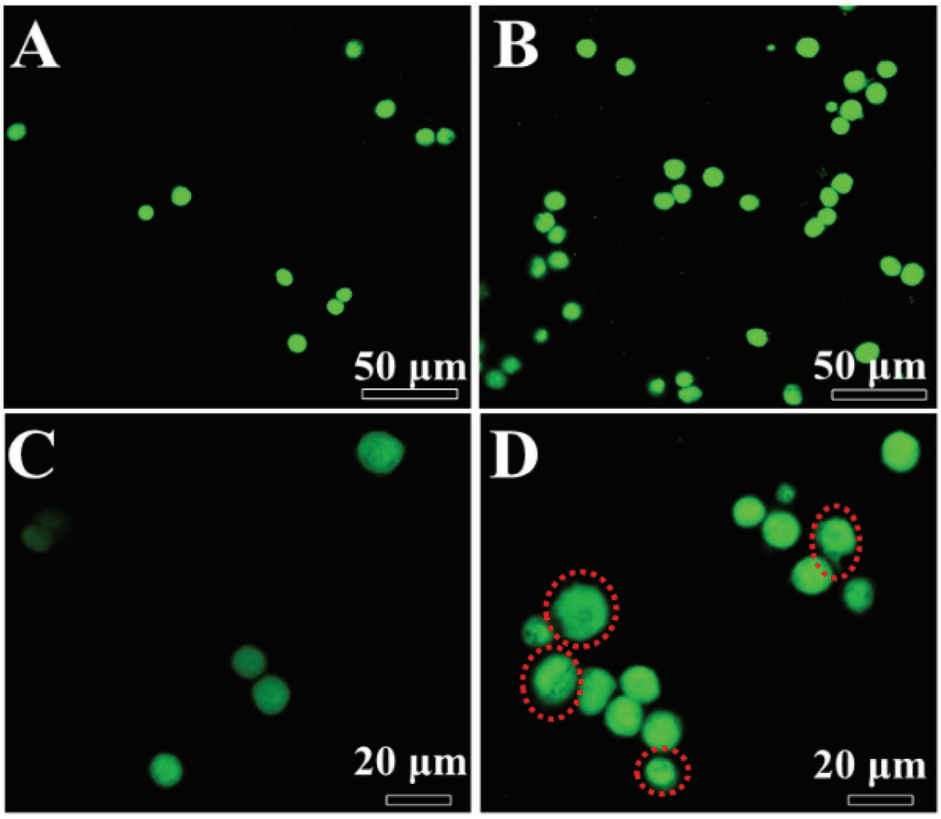

Figure 7. Fluorescent images of calcein-AM cell staining. A,C) MDA-MB-231 cells on the TNAs/PDA/PEG-FA electrode and B,D) MDA-MB-231 cells on the TNAs/PDANSs/PDA/PEG-FA electrode (EX = 488 nm).

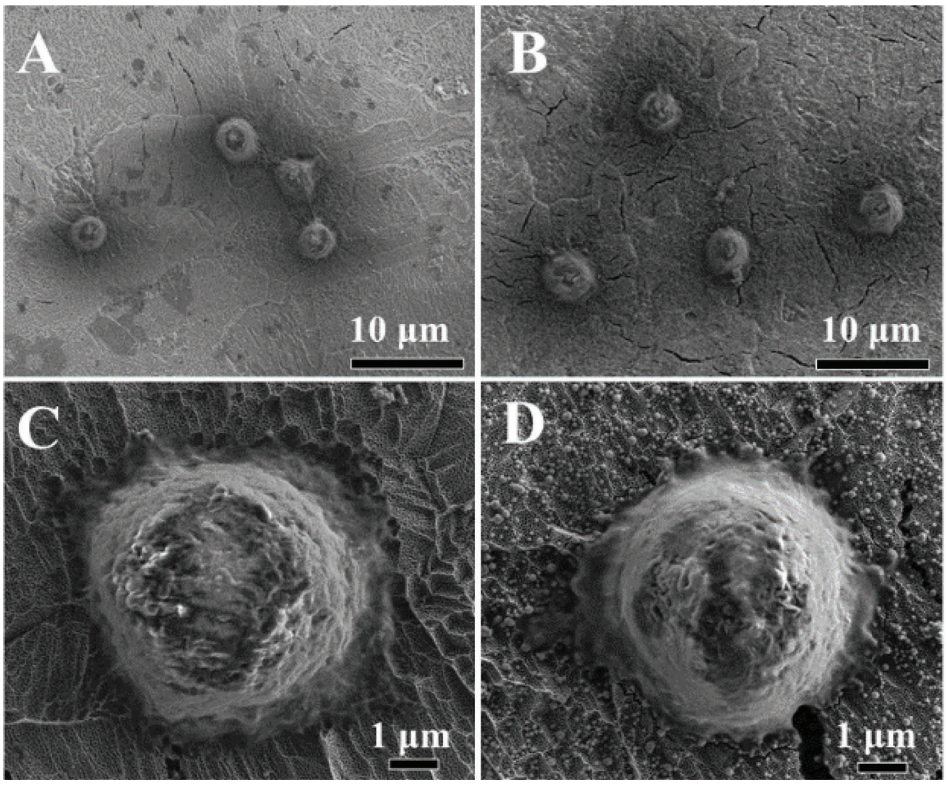

Figure 8. SEM images of A,C) TNAs/PDA/PEG-FA/Cells and B,D) TNAs/PDANSs/PDA/PEG-FA/Cells.

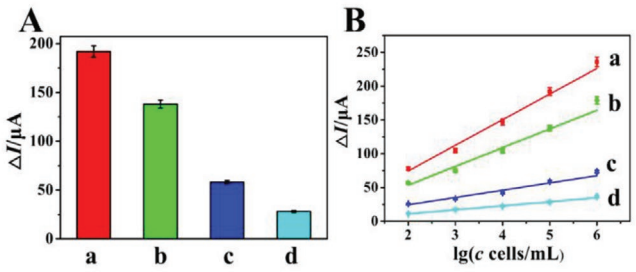

Figure 9. A) Photocurrent response of different cells at the same concentration (1.0×10^5 cells). B) Working curve of photocurrent response of TNAs/PDANSs/PDA/PEG-FA electrodes at the same concentration (1.0×10^2, 1.0×10^3, 1.0×10^4, 1.0×10^5, and 1.0×10^6) in different cells: a) MDA-MB-231 cells, b) MCF-7 cells, c) A549 cells, and d) HUVEC cells.

heterogeneity of cancer cells. The PEC cytosensing with high sensitivity provides facile label-free methods for the evaluation of expressing differentiation of FR on cells based on the PEC responses. Both cancer cells (MDA-MB-231, MCF-7, and A549) and normal tissue cells (HUVEC) were adopted for the comparison of their PEC responses (**Figure 9**A). The larger PEC responses of MDA-MB-231, MCF-7, and A549 than HUVEC indicate the overexpression of FR on cancer cells. The expressing differentiation of FR on three types of cancer cells can also be obtained based on the slope of the PEC responses (Figure 9B), that is, MDA-MB-231 > MCF-7 > A549, which in consistent with the reported results.[23,51]

3. Conclusion

In this work, we designed a new type of label-free antifouling PEC biosensor, which can effectively capture and detect MDA-MB-231 cells with a wide detection range and low detection limit. Moreover, the PDANSs were modified on TNAs to construct "sphere-on-tube" hierarchical nanostructure and then the PDA was coated on the surface of hierarchical nanostructure to enhance PEC responses. Apparently, the addition of PEG and FA improved the antifouling performance and specificity. More importantly, the PEC biosensor can also be used to evaluate FR expressed on the cell membrane. This strategy has great potential in cell capture and detection, indicating broad application prospects in clinical applications.

4. Experimental Section

Preparation of PEC Biosensor: In detail, the titanium pieces were successively treated with ultrasound in ultrapure water, acetone, and ethanol for 30 min. Titanium pieces were anodized in ethylene glycol (EG) containing 0.3 wt% NH_4F and 2% by volume H_2O at the constant voltage of 40 V for 1 h. Finally, the obtained sample was calcined in a muffle furnace at 450 °C for 1 h to obtain highly ordered TiO_2 nanotube arrays (TNAs).

PDANSs were prepared through oxidative polymerization of dopamine hydrochloride (DA). 100 mg of DA was added into a mixture of 100 mL Tris buffer (pH = 8.8) and 50 mL isopropyl alcohol. After stirring for 24 h, the resulting product was collected by centrifugation at 9000 rpm for 20 min and washed with water for five times to remove unreacted substances. Ultimately, it was redispersed into 5 mL ultrapure water for further using.

The oxidized titanium dioxide nanotube was cut into 0.6×3 cm^2 and acted as a working electrode. Then, the electrode was immersed in 2.5 mg mL^{-1} PDANSs solution for 60 min and washed the electrode with ultrapure water. Subsequently, the prepared TNAs/PDANSs was soaked in the newly prepared DA solution (2 mg mL^{-1}) prepared with Tris-HCl buffer solution (pH = 8.5, 0.1 M) for 150 min. Afterward, the electrode was washed with the Tris-HCl buffer solution. Finally, the TNAs/PDANSs/PDA electrode was prepared.

The NH_2-polyethylene glycol (PEG) solution (1 mg mL^{-1}) was prepared with Tris-HCl buffer solution (pH = 8.5, 0.1 M). Then the TNAs/PDANSs/PDA electrode was immersed into the above solution for 60 min. Subsequently, the TNAs/PDANSs/PDA/PEG electrode was immersed in the FA solution for 60 min under dark conditions. Similarly, the obtained TNAs/PDANSs/PDA/PEG-FA electrode was rinsed with phosphate buffered saline (PBS) buffer solution. Eventually, the PEC sensing platform was successfully prepared.

Antifouling Performance of PEC Biosensor: The PEC current and EIS changes before and after protein contamination were used to evaluate the prepared sensing platform. The experiment of photocurrent response test was acquired under excitation light at a wavelength of 557 nm on a PEC workstation with a bias voltage of 0 V at room temperature. EIS testing was carried out in electrolyte solution containing 5 mmol L^{-1} $[Fe(CN)_6]^{3-/4-}$ and 0.1 mol L^{-1} KCl with AC amplitude 5 mV and the frequency range was set as 10^{-1}–10^5 Hz without light. And then, the electrode was immersed into 0.5 mg mL^{-1} protein (Hb, IgG, and human serum) solution for 30 min. Obviously, the PEC current and EIS diagram before and after protein have barely change, indicating the constructed sensor had good antifouling performance.

PEC Detection for the Target: The sensor preparation and sensing conditions were selected. By optimizing the voltage and time of anodizing, the stable tubular structure of the electrode was ensured. The optimum performance was determined by screening AA, pH, PDANSs, PDA, and PEG concentrations (Supporting Information). The TNAs/PDANSs/PDA/PEG-FA electrode was soaked in MDA-MB-231 cell suspension of different concentrations and subjected to magnetically stirring for 30 min. After that, the above electrode was washed for further detection.

Cell Culture and Fluorescent Staining: The breast cancer cell line (MCF-7, MDA-MB-231), human squamous-cell lung carcinoma cell line A549, and human umbilical vein endothelial cells (HUVEC cell line 20170811-2, DSMZ, from Chi Scientific) were trained in Dulbecco's modified eagle medium or Roswell Park Memorial Institute (RPMI)-1640 containing fetal bovine serum (10%), penicillin and streptomycin (1%), and incubated in an incubator with CO_2 concentration of 5.0% at 37 °C. In confluence reaches 80%, cells were digested with 0.25% trypsin-ethylene diamine tetraacetic acid (EDTA), and collect immediately after centrifugation at 1000 rpm for 10 min. Subsequently, cells were redistributed with PBS (1 mL, pH = 7.4) buffer solution to form a stable cell suspension. Afterward, 20 μL of cell suspension was taken and incubated on different platforms for 30 min. Finally, the living cells captured on the electrode surface were stained with calcein-acetoxymethyl ester (AM) (5 μg mL^{-1}, 10 μL).

A Zeiss laser confocal microscope (LSM880) was used to record photoluminescence at room temperature in the range of 430–750 nm with an excitation wavelength of 488 nm. The scanning resolution was 512×512, the eyepiece was 10 X, and the field of view was 25 mm.

Scanning Electron Microscopy (SEM) Observation: First, the MDA-MB-231 cells were incubated for 1 h. Then, the electrode was carefully washed three times with PBS buffer solution to remove the medium. Subsequently, the cells were fixed with 4% paraformaldehyde at 4 °C for 30 min, washed with PBS buffer solution. Afterwards, the cells were dehydrated in different concentrations of ethanol (20%, 40%, 60%, 80%, 95%, 100%) for 15 min each time. Eventually, the cells morphology was observed by SEM.

Supporting Information

Supporting Information is available from the Wiley Online Library or from the author.

Acknowledgements

This study was financially supported by the Shandong Provincial Natural Science foundation (ZR2020YQ13), a Project of Shandong Province Higher Educational Youth Innovation Science and Technology Program (2020KJC008), and Jinan Scientific Research Leader Workshop Project (2020GXRC048).

Conflict of Interest

The authors declare no conflict of interest.

Data Availability Statement

The data that support the findings of this study are available from the corresponding author upon reasonable request.

Keywords

antifouling, folate receptors, hierarchical nanostructures, polydopamine nanospheres, polyethylene glycol, TiO_2 nanotube arrays

Received: March 15, 2021
Revised: May 6, 2021
Published online:

[1] H. Kim, W. J. Muller, *Exp. Cell. Res.* **1999**, *253*, 78.
[2] C. Muller, R. Schibli, *J. Nucl. Med.* **2011**, *52*, 1.
[3] T. J. Chen, T. H. Cheng, Y. C. Hung, K. T. Lin, G. C. Liu, Y. M. Wang, *J. Biomed. Mater. Res., Part A* **2008**, *10*, 165.
[4] P. Delcanale, D. Porciani, S. Pujals, A. Jurkevich, A. Chetrusca, K. D. Tawiah, *Angew. Chem., Int. Ed.* **2020**, *59*, 18546.
[5] W. Cheng, L. Ding, J. Lei, S. Ding, H. Ju, *Anal. Chem.* **2008**, *80*, 3867.
[6] A. Tamashevski, Y. Harmaza, R. Viter, D. Jevdokimovs, R. Poplausks, E. Slobozhanina, L. Mikoliunaite, D. Erts, A. Ramanaviciene, A. Ramanavicius, *Talanta* **2019**, *200*, 378.
[7] J. Xu, Y. Hu, S. Wang, X. Ma, J. Guo, *Analyst* **2020**, *145*, 2058.
[8] T. Zheng, J. J. Fu, L. Hu, F. Qiu, M. Hu, J. J. Zhu, *Anal. Chem.* **2013**, *85*, 5609.
[9] C. Gu, P. Gai, X. Liu, J. Liu, F. Li, *Sens. Actuators, B* **2018**, *270*, 1.
[10] H. Cao, D. P. Yang, D. Ye, X. Zhang, X. Fang, S. Zhang, *Biosens. Bioelectron.* **2015**, *68*, 329.
[11] Y. Qiu, B. Zhou, X. Yang, D. Long, Y. Hao, P. Yang, *ACS Appl. Mater. Interfaces* **2017**, *9*, 16848.
[12] E. Han, L. Ding, H. Lian, H. Ju, *Chem. Commun.* **2010**, *46*, 5446.
[13] W. Liang, Y. Zhuo, C. Xiong, Y. Zheng, Y. Chai, R. Yuan, *Anal. Chem.* **2015**, *87*, 12363.
[14] W. W. Zhao, L. Zhang, J. J. Xu, H. Y. Chen, *Chem. Commun.* **2012**, *48*, 9456.
[15] R. Wu, G. C. Fan, L. P. Jiang, J. J. Zhu, *ACS Appl. Mater. Interfaces* **2018**, *10*, 4429.
[16] L. Cui, J. Z. Shen, S. Y. Ai, X. L. Wang, *Biosens. Bioelectron.* **2020**, *168*, 112545.
[17] S. Zhang, H. Bai, J. Pi, P. Yang, J. Cai, *Anal. Chem.* **2015**, *87*, 4797.
[18] H. Chen, Y. Hou, Z. Ye, H. Wang, K. Koh, Z. Shen, *Sens. Actuators, B* **2014**, *201*, 433.
[19] L. Feng, Y. Chen, J. Ren, X. Qu, *Biomaterials* **2011**, *32*, 2930.
[20] Z. Wang, J. Li, W. Tu, H. Wang, Z. Wang, Z. Dai, *ACS Appl. Mater. Interfaces* **2020**, *12*, 26905.
[21] M. Fernández, F. Javaid, V. Chudasama, *Chem. Sci.* **2018**, *9*, 790.
[22] L. E. Kelemen, *Int. J. Cancer* **2006**, *119*, 243.
[23] L. Du, W. Chen, J. Wang, W. Cai, S. Kong, C. Wu, *Sens. Actuators, B* **2019**, *301*, 127073.
[24] I. A. Jammaz, B. A. Otaibi, S. Amer, N. A. Hokbany, S. Okarvi, *Nucl. Med. Biol.* **2012**, *39*, 864.
[25] J. Soleymani, M. Hasanzadeh, N. shadjou, M. H. Somi, A. Jouyban, *Trends Anal. Chem.* **2020**, *125*, 115834.
[26] M. Li, H. Ding, M. Lin, F. Yin, L. Song, X. Mao, *J. Am. Chem. Soc.* **2019**, *141*, 18910.
[27] H. Cui, B. Wang, W. Wang, Y. Hao, C. Liu, K. Song, W. W. Zhao, Z. Y. Ma, D. Y. Yan, J. J. Xu, H. Y. Chen, *Anal. Chem.* **2012**, *84*, 10518.
[28] D. Chen, H. Zhang, X. Li, J. Li, *Anal. Chem.* **2010**, *82*, 2253.
[29] Y. An, L. Tang, X. Jiang, H. Chen, M. Yang, L. Jin, *Chem. - Eur. J.* **2010**, *16*, 14439.
[30] Q. Kang, L. Yang, Y. Chen, S. Luo, L. Wen, Q. Cai, *Anal. Chem.* **2010**, *82*, 9749.
[31] N. Liu, J. Song, Y. Lu, J. J. Davis, F. Gao, X. Luo, *Anal. Chem.* **2019**, *91*, 8334.
[32] S. Ramanavicius, A. Ramanavicius, *Sensors* **2020**, *20*, 6833.
[33] G. C. Fan, Z. Li, Y. Lu, L. Ma, H. Zhao, X. L. Luo, *Sens. Actuators, B* **2019**, *299*, 126996.
[34] G. Loget, J. E. Yoo, A. Mazare, L. Wang, P. Schmuki, *Electrochem. Commun.* **2015**, *52*, 41.
[35] J. Li, X. Li, Q. Zhao, Z. Jiang, M. Tadé, S. Wang, *Sens. Actuators, B* **2018**, *255*, 133.
[36] B. Fan, Q. Fan, L. Hu, M. Cui, X. Wang, H. Ma, *ACS Appl. Mater. Interfaces* **2020**, *12*, 1877.
[37] Q. Kang, S. Liu, L. Yang, Q. Cai, C. A. Grimes, *ACS Appl. Mater. Interfaces* **2011**, *3*, 746.
[38] L. Niu, L. Meng, Q. Lu, *Macromol. Biosci.* **2013**, *13*, 735.
[39] D. R. Dreyer, D. J. Miller, B. D. Freeman, D. R. Paul, C. W. Bielawski, *Langmuir* **2012**, *28*, 6428.
[40] J. Varshosaz, F. Hassanzadeh, H. Sadeghi Aliabadi, M. Nayebsadrian, M. Banitalebi, M. Rostami, *Biomed. Res. Int.* **2014**, *14*, 525684.
[41] R. O. Ogbodu, E. Antunes, T. Nyokong, *Polyhedron* **2013**, *60*, 59.
[42] H. Lee, S. M. Dellatore, W. M. Miller, P. B. Messersmith, *Science* **2007**, *318*, 426.
[43] E. Balaur, J. M. Macak, L. Taveira, P. Schmuki, *Electrochem. Commun.* **2005**, *7*, 1066.
[44] H. J. Nam, B. Kim, M. J. Ko, M. S. Jin, J. M. Kim, D. Y. Jung, *Chem. - Eur. J.* **2012**, *18*, 14000.
[45] N. Hui, X. Sun, S. Niu, X. Luo, *ACS Appl. Mater. Interfaces* **2017**, *9*, 2914.
[46] A. Ramanavicius, A. Finkelsteinas, H. Cesiulis, *Bioelectrochemistry* **2010**, *79*, 11.
[47] H. Ma, J. Hyun, P. Stiller, A. Chilkoti, *Adv. Mater.* **2004**, *16*, 338.
[48] H. Ma, F. Qi, B. Fan, Z. Yong, D. Fan, W. Dan, *Langmuir* **2018**, *34*, 7744.
[49] Y. Y. Liu, Y. Zhao, Z. Zhu, Z. Xing, H. Ma, Q. Wei, *Anal. Chim. Acta* **2017**, *963*, 17.
[50] X. L. Wang, X. J. Wang, S. S. Chen, M. Q. Ye, C. L. Zhang, Y. Z. Xian, *Anal. Chem.* **2020**, *92*, 3111.
[51] H. H. Cai, J. Pi, X. Y. Lin, B. L. Li, A. Q. Li, P. H. Yang, J. Y. Cai, *Biosens. Bioelectron.* **2015**, *74*, 165.

